Overview of ALICE results on light flavour hadron production

V G Riabov[1,2] for the ALICE Collaboration

[1] PNPI of NRC "Kurchatov Institute", 1, mkr. Orlova roshcha, Gatchina, 188300, Russia
[2] National Research Nuclear University MEPhI (Moscow Engineering Physics Institute), Kashirskoe highway 31, Moscow, 115409, Russia

E-mail: riabovvg@pnpi.nrcki.ru

Abstract. Light flavour hadrons are copiously produced in hadronic and heavy-ion interactions and bring a wealth of information about properties of the produced medium and reaction dynamics. Having different masses, quark content and lifetimes, light flavour hadrons do not only serve as general observables in the soft sector, but also play an important role as high transverse momentum probes and signatures of the onset of collectivity in high-multiplicity collisions of small and large systems. In this manuscript, we review the most recent ALICE results on the production of different light-flavour hadrons, including transverse momentum spectra, yields, nuclear modification factors and particle ratios in pp, p-Pb, Xe-Xe and Pb-Pb collisions at LHC energies.

1. Introduction

Studies of light flavor hadron production play an important role in understanding the physics of heavy-ion collisions. Production of light flavor hadrons containing strange quarks is measured to study strangeness enhancement from pp to p-Pb and Xe-Xe/Pb-Pb collisions and its dependence on the particle strangeness content and whether it is present for particles with hidden strangeness. The production of short-lived resonances with lifetimes comparable to that of the fireball is measured to study rescattering and regeneration processes in the dense hadronic medium. Transverse momentum spectra and particle ratios probe the particle production mechanisms in different kinematic regions, carry information about interplay of the radial flow and parton recombination at intermediate transverse momenta (p_T) as well as parton energy loss at high p_T. In this paper we review selected ALICE results on light flavor hadron production and compare them to lower energy experiments and theoretical model predictions where available.

2. Results and discussions

Figure 1 shows p_T-integrated particle yields measured in 0-10% central Pb-Pb collisions at $\sqrt{s_{NN}}$ = 2.76 [1] and 5.02 TeV compared to three grand-canonical thermal model predictions [2,3]. The models, which assume hadron production at chemical equilibrium, correctly reproduce most of the measured yields with a chemical freeze-out temperatures of ~ 156 MeV at 2.76 TeV and ~ 153 MeV at 5.02 TeV, which are consistent within uncertainties. The models also reproduce production of nuclei and hyper-nuclei although their binding energies are much smaller than the extracted values of the chemical freeze-out temperatures. There are several outliers, for example, $K^*(892)^0$ is predicted to have

a larger yield and the difference is explained by loss of $K^*(892)^0$ signal in the haronic phase as discussed later in the text. For this reason $K^*(892)^0$ is not included in the fit. There is also a tension for protons and multi-strange baryons, which may have different reasons such as baryon annihilation, interactions in the hadron gas or feed-downs from excited hadronic states etc. Overall, thermal models are quite successful and describe hadron production in seven orders of magnitude of d*N*/dy.

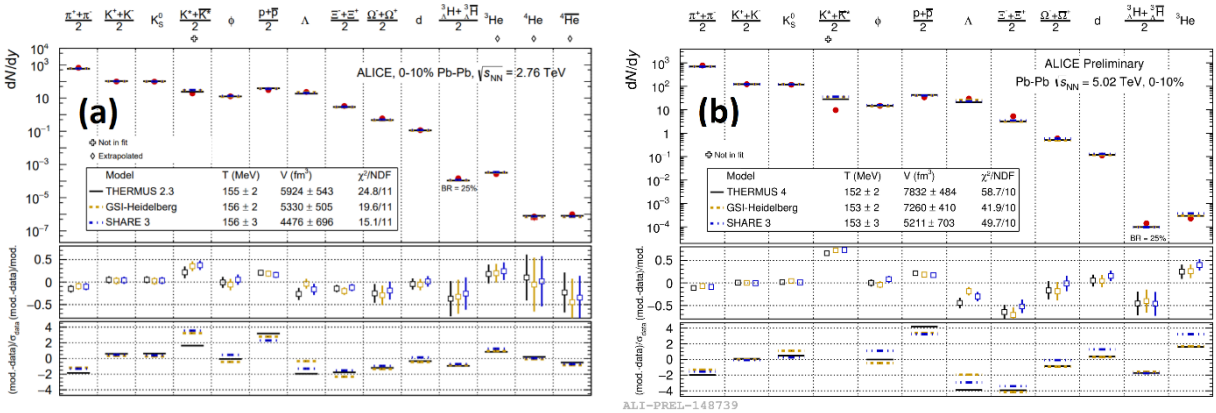

Figure 1. Particle integrated yields compared to three grand-canonical thermal model predictions in 0-10% central Pb-Pb collisions at $\sqrt{s_{NN}}$ = 2.76 TeV (a) and 5.02 TeV (b).

Resonances, which are excited hadronic states with short lifetimes probe the existence of particle rescattering and regeneration in the hadronic phase, which can either reduce or enhance the resonance yields measured in hadronic decay channels. In this picture the resonance yields in the final state are defined by the resonance yields at chemical freeze-out, their lifetimes, hadronic phase lifetime and by scattering cross sections. The most often measured resonances are ρ(770), $K^*(892)$, Λ(1520), $\Xi(1530)^0$, and ϕ(1020), which cover a wide range of the lifetimes from 1.3 fm/*c* for ρ(770) meson up to 46.2 fm/*c* for ϕ(1020) meson [4]. Figure 2 shows ratios of the resonance yields to yields of quasi-stable hadrons having similar constituent quarks. These are $\rho(770)^0/\pi$, $K^*(892)^0/K$, $\Sigma(1385)^{\pm}/\Lambda$, $\Lambda(1520)/\Lambda$, $\Xi(1530)^0/\Xi^-$ and ϕ(1020)/K ratios shown as a function of the charged particle multiplicity in pp, p-Pb, Xe-Xe (where available) and Pb-Pb collisions at LHC energies and in pp and Au-Au collisions at $\sqrt{s_{NN}}$ = 200 GeV measured by the STAR experiment at RHIC [5-7]. One can see that the ratios do not show any significant collision energy dependence. The ratios are suppressed in central heavy-ion collisions for the short-lived resonances with lifetimes of $\tau < 20$ fm/*c* compared to pp and peripheral heavy-ion collisions. Ratios are also overestimated by thermal model predictions. Ratios for longer-lived resonances are not suppressed and, for example, ϕ(1020) behaves as a stable particle. Results support the existence of a hadronic phase that lives long enough to cause a significant reduction of the reconstructed yields of short lived resonances. The observed modifications of the ratios are well reproduced by EPOS3 event generator with UrQMD used as hadronic phase afterburner [8,9]. The measurements allowed to put a lower limit for the hadronic phase lifetime, $\tau_{had} > 2$ fm/*c* [10].

Originally, strangeness enhancement was considered as a signature of QGP formation in heavy-ion collisions [11]. However interpretation of strangeness production results is not straightforward. Left panel of Figure 3 shows ratios of the yields of particles containing one or more *s*-quarks to the yield of charged pions measured as a function of multiplicity in pp, p-Pb, Xe-Xe and Pb-Pb collisions [12]. A smooth evolution of the ratios with multiplicity is observed for all collision systems at different energies. With these measurements ALICE for the first time demonstrates presence of the strangeness enhancement is high multiplicity collisions of small systems. In all systems, the enhancement increases with strangeness content of the particle. Thermal model predictions describe measurements in central heavy-ion collisions, which are consistent with the highest multiplicity results in p-Pb. Strange

resonances such as $\Sigma(1385)^{\pm}$ and $\Xi(1530)^{0}$ also show increasing patterns depending on the strangeness content, which is consistent with observations for ground-state hadrons [13].

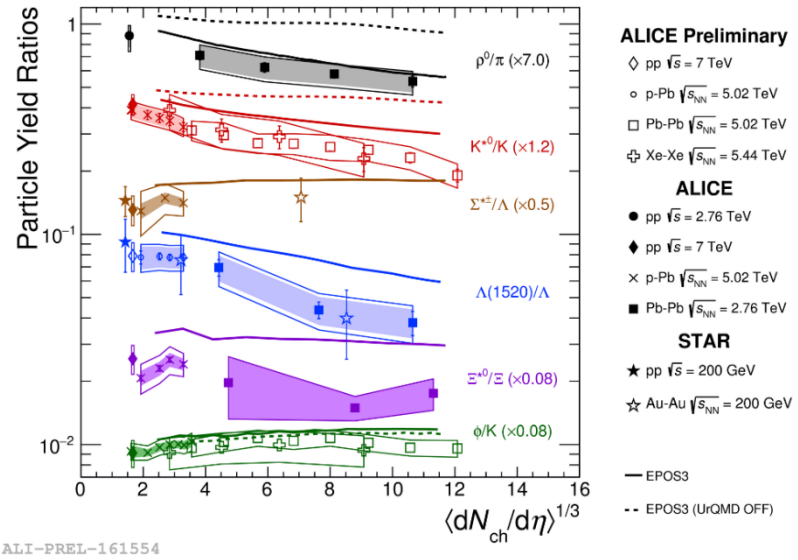

Figure 2. Summary of particle yield ratios, $\rho(770)^0/\pi$, $K^*(892)^0/K$, $\Sigma(1385)^{\pm}/\Lambda$, $\Lambda(1520)/\Lambda$, $\Xi(1530)^0/\Xi^-$ and $\phi(1020)/K$ as a function of multiplicity in pp, p-Pb, Xe-Xe, and Pb-Pb collisions at $\sqrt{s_{NN}}$ = 2.76–7 TeV and in pp and Au-Au collisions at $\sqrt{s_{NN}}$ = 200 GeV, with comparison to EPOS3.

$\phi(1020)$ meson is a particle that consists of $s\bar{s}$ pair and it has a hidden strangeness. For this reason it is well suited to study origin of the strangeness enhancement. Right panel of Figure 3 shows $2{\cdot}\phi(1020)/\pi$ ratio as a function of multiplicity in pp, p-Pb, Xe-Xe and Pb-Pb collisions at different energies. Although $\phi(1020)$ is not a strange particle it behaves similar to particles with open strangeness. Ratio $2{\cdot}\phi(1020)/\pi$ increases with multiplicity and saturates in high multiplicity p-Pb collisions. The observed $\phi(1020)$ meson enhancement in small systems is not expected for canonical suppression scenario. Figure 2 shows that $\phi(1020)/K$ ratio does not depend on multiplicity in different collision systems within uncertainties. $\Xi/\phi(1020)$ ratio shown in the right panel of Figure 3 is also fairly flat as a function of multiplicity. It indicates that $\phi(1020)$ meson behaves as a particle with an effective strangeness of 1 or 2.

Left panel of Figure 4 shows p_T-differential p/π and Λ/K_s^0 ratios measured in the highest and lowest multiplicity pp, p-Pb and Pb-Pb collisions [14]. A very similar behavior of the ratios is observed for all systems, there is a decrease of the ratio at low p_T, enhancement at intermediate p_T and full consistency of the ratios at higher momenta. The enhancement of the baryon-to-meson ratios in heavy-ion collisions at intermediate transverse momentum is known as a baryon puzzle, which predominantly originates from the radial flow and parton recombination. However there is no unique explanation for similar enhancement observed in high multiplicity collisions of small systems. Qualitatively, increase of the ratios in pp collisions is reproduced by Pythia8 with color reconnection and DIPSY with color ropes. Details of the baryon puzzle can be studied by measuring baryon-to-meson ratios for particles of similar masses. Right panel of Figure 4 shows p_T-differential $p/\phi(1020)$ ratios measured in central Xe-Xe and semi-central Pb-Pb collisions having similar multiplicities. Results are shown with red markers. Black and blue points show p/π and Λ/K_s^0 ratios in the same systems. One can see that baryon-to-meson ratios for particles of similar masses are flat at intermediate momentum. It indicates that shapes of the particle p_T spectra are determined by particle masses as expected from hydrodynamical models. However, recombination models cannot be completely ruled out, some of them predict a similar effect [15].

Collective effects at high-p_T are studied with a so called nuclear modification factor, R_{AA}, which is equal to the ratio of the particle yields in heavy-ion and pp collisions scaled by the corresponding number

of binary inelastic nucleon-nucleon collisions. Figure 5 shows nuclear modification factors for charged hadrons and $K^*(892)^0$ meson in Xe-Xe and Pb-Pb collisions at similar energies of $\sqrt{s_{NN}}$ = 5.44 TeV and

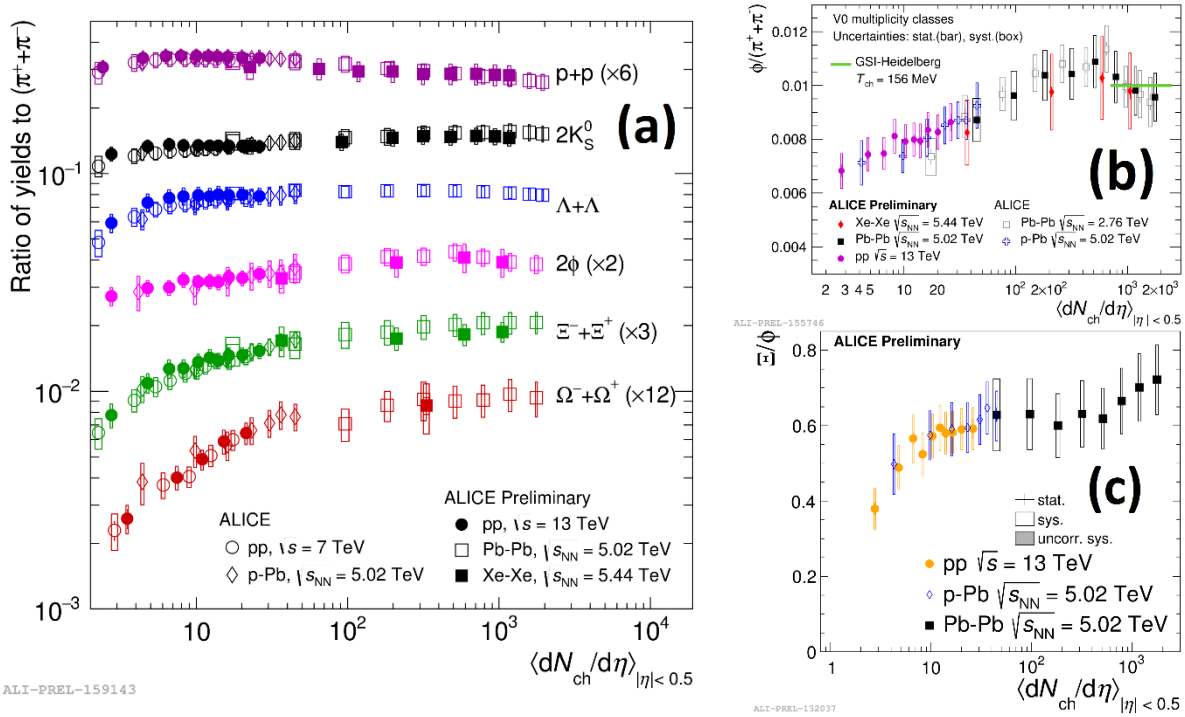

Figure 3. Ratios of particle p_T-integrated yields measured as a function of multiplicity across different collision systems: (a) 2·p/π, 2·K^0_S/π, 2·Λ/π, 2·φ(10120)/π, 2·Ξ/π and 2·Ω/π in pp at $\sqrt{s}$ = 7 and 13 TeV, p-Pb and Pb-Pb at $\sqrt{s_{NN}}$ = 5.02 TeV, Xe-Xe at $\sqrt{s_{NN}}$ = 5.44 TeV; (b) 2·φ(1020)/π in pp at $\sqrt{s}$ = 13 TeV, p-Pb at $\sqrt{s_{NN}}$ = 5.02 TeV, Pb-Pb at $\sqrt{s_{NN}}$ = 2.76 and 5.02 TeV, Xe-Xe at $\sqrt{s_{NN}}$ = 5.44 TeV; (c) Ξ/φ(1020) in pp at $\sqrt{s}$ = 13 TeV, p-Pb and Pb-Pb at $\sqrt{s_{NN}}$ = 5.02 TeV.

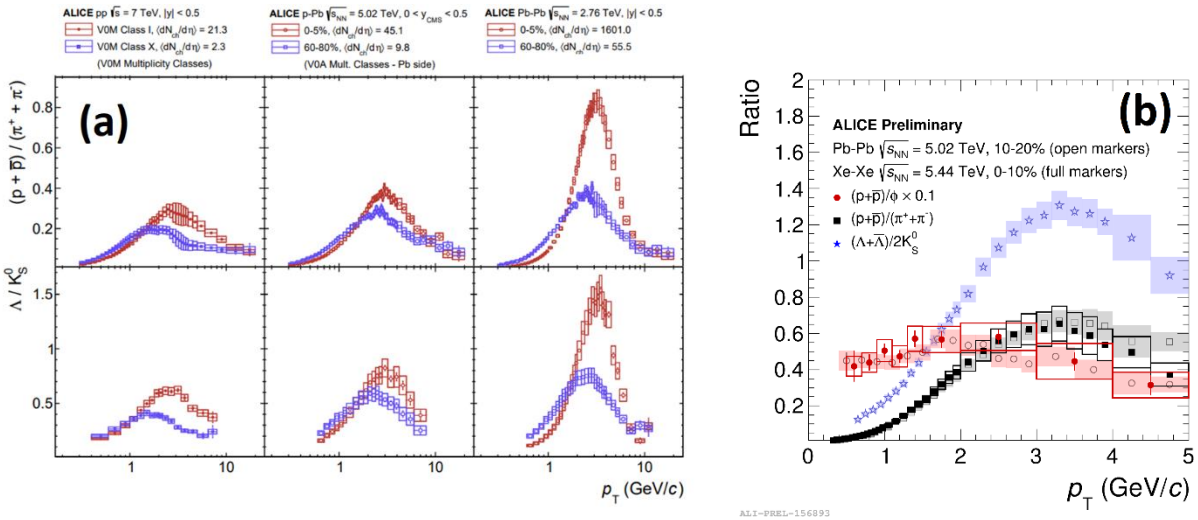

Figure 4. : Particle ratios as a function of transverse momentum in different collision systems: (a) p/π (top) and Λ/K_s^0 (bottom) in the highest (red) and lowest (blue) multiplicity bins, pp at $\sqrt{s}$ = 7 TeV, p-Pb at $\sqrt{s_{NN}}$ = 5.02 TeV and Pb-Pb at $\sqrt{s_{NN}}$ = 2.76 TeV; (b) p/φ(1020), p/π and Λ/K_s^0 ratios in central

heavy-ion collisions at similar multiplicities, 10-20% central Pb-Pb at $\sqrt{s_{NN}}$ = 5.02 TeV and 0-10% central Xe-Xe at $\sqrt{s_{NN}}$ = 5.44 TeV.

5.02 TeV, respectively, and similar multiplicities. The R_{AA} factors are consistent for both systems, suggesting an interplay of the system geometry and path length dependence of the parton energy loss. The R_{AA} factors measured for light hadrons in Pb-Pb collisions at $\sqrt{s_{NN}}$ = 2.76 TeV and 5.02 TeV are also consistent within uncertainties. Production of all light hadrons is similarly suppressed at high transverse momenta, p_T > 10 GeV/c, in central heavy-ion collisions at the LHC suggesting that suppression occurs at partonic level.

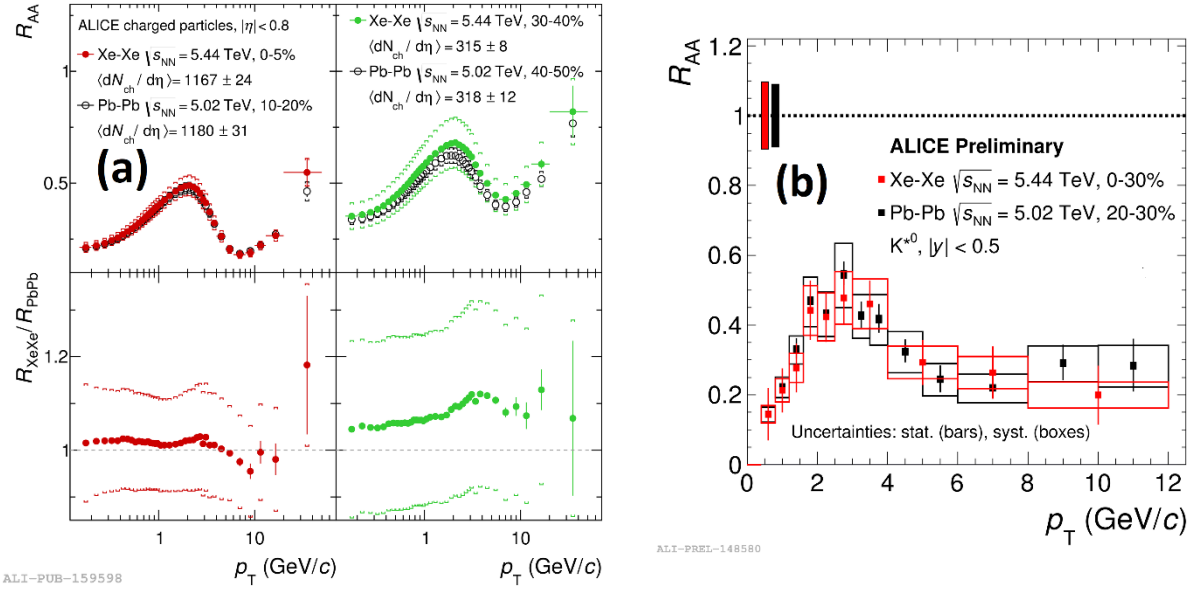

Figure 5. : Comparison of nuclear modification factors (R_{AA}) for hadrons in Xe-Xe collisions at $\sqrt{s_{NN}}$ = 5.44 TeV and Pb-Pb collisions at $\sqrt{s_{NN}}$ = 2.76 TeV for centrality bins having similar number of participants: (a) charged hadrons in 0-5% (10-20%) and 30-40% (40-50%) central Xe-Xe (Pb-Pb) collisions; (b) $K^*(892)^0$ in 0-30% (20-30%) central Xe-Xe (Pb-Pb) collisions.

Acknowledgements
This work was partially supported by the National Research Nuclear University MEPhI in the framework of the Russian Academic Excellence Project (contract No. 02.a03.21.0005, 27.08.2013).

References

[1] Acharya S *et al.* 2018 *Nucl. Phys.* A **971** 1-20
[2] Floris M 2014 *Nucl. Phys.* A **931** 103-112
[3] Andronic A, Braun-Munzinger P, Redlich K, Stachel J 2017 *J. Phys. Conf. Ser.* **779** no.1 012012
[4] Tanabashi M *et al.* 2018 *Phys. Rev.* D **98** 030001
[5] Adams J *et al.* 2005 *Phys. Rev.* C **71** 064902
[6] Abelev B *et al.* 2006 *Phys. Rev. Lett.* **97** 132301
[7] Adams J *et al.*, 2005 *Phys. Lett.* B **612** 181–189
[8] Knospe A, Markert C, Werner K, Steinheimer J, Bleicher M 2016 *Phys. Rev.* C **93** no. 1 014911
[9] Bass S A *et al.* 1998 *Prog. Part. Nucl. Phys.* **41** 255–369
[10] Abelev B *et al.* 2015 *Phys. Rev.* C **91** 024609
[11] Rafelsky J, Muller B 1982 *Phys. Rev. Lett.* **48** 1066, Erratum: 1986 *Phys. Rev. Lett.* **56** 2334
[12] Adam J *et al.* 2017 *Nature Phys.* **13** 535-539

[13] Adamova D *et al.* 2017 *Eur. Phys. J.* C **77** no.6 389
[14] Acharya S *et al.* 2018 *Preprint* 807.11321
[15] Greco Vm Minissale V, Scardina F 2015 *Phys. Rev.* C **92** no.5 054904